Fermi National Accelerator Laboratory

TM-1354
1100.060

Radiation Shielding for 250 MeV Protons

Miguel Awschalom

Fermi National Accelerator Laboratory
P.O. Box 500
Batavia, IL 60510 USA

September 23, 1985
Revised April 1, 1987

Operated by Universities Research Association Inc. under contract with the United States Department of Energy

TM-1354
1100.060
Rev.4/1/87

RADIATION SHIELDING FOR 250 MeV PROTONS

Miguel Awschalom

September 23, 1985

Accelerator Division Headquarters

INTRODUCTION

This technical memorandum was written for the benefit of the personnel of Loma Linda University Medical Center, Proton Therapy Facility, who have the responsibility of designing the radiation shielding against neutron fluences created when 70-250 MeV protons interact with matter.

These few pages provide a guide to shielding design given in just enough detail to make the presentations plausible but without any attempt at being either pedagogical or complete. There is, however, enough material in this TM to allow the perseverant to trace the source of the calculations to their origins.

This note is naturally divided into two parts: walls and roof shielding, and neutron dose leakage through labyrinths.

In the 100 to 400 MeV proton kinetic energy region there is precious little data on neutron dose attenuation in thick shields and very few calculations of the type needed for shielding calculations in a building where all polar production angles, from 0° to 180° are important. The only

clean neutron flux attenuation experiment is one at 200 MeV carried out by Distenfeld[1] at Brookhaven National Laboratory. This experiment was carried out in a water tank. The measurements were made at 90° to the beam and consisted in activating the following samples:

$^{23}Na\ (n,\gamma)\ ^{24}Na$ $\qquad$ $^{12}C(n,\ 2n)^{11}C$

$^{27}Al\ (n,\alpha)^{24}Na$ $\qquad$ Cl(n,various)various

Other experimental data stems from the measurements made at Harvard by Wachter et al.[2] These measurements essentially confirm the goodness of fit of Bertini's[3] calculations of primary reactions to the real world. Bertini's calculations were later statistically analyzed and parametrized by Alsmiller et al.[4]

The last supporting experimental results are the work of Ban et al[5]. In a good geometry set-up they measured the mean free path of neutrons created by 500 MeV protons in steel at zero and near hundred degrees. These they compare with extrapolations of calculations made by several authors.

Next, we will review briefly some calculations that have been made using the Bertini intranuclear cascade calculations[3] and Alsmiller et al[4] parametrizations.

Alsmiller et al[6] analyzed Distenfeld[1] results successfully, see figure 1. The calculation assumes that 200 MeV protons are stopped in water. Thus, the work of Alsmiller, Santoro and Barish becomes the best documented

one and, the basis for some simple extrapolation calculations that are presented later on. Alsmiller's neutron dose attenuation calculations in ordinary concrete for 200 MeV stopping in aluminum are shown in figure 2.

There is an older calculation by Alsmiller et al[7]. However, this is a straight ahead calculation, averaged over the forward hemisphere and it is of no practical value in shielding design applications. The incident neutron spectrum is that of 200 MeV protons striking a thick copper target and then taking the cascade neutrons produced in the 30°-60° polar angle.

Calculations were also made in a unpublished technical memorandum by H.Lundgvist[8]. Lundqvist compares two neutron energy spectra from targets bombarded with 160 MeV protons at the Harvard Cyclotron Laboratory by Wachter[5] et al with his calculations. The agreement is very good, see figures 3 and 4. In these notes Lundqvist also presents a comparison of calculations and measurements at 185 MeV. The measurements had been made by a team from CERN. However, the results of the measurements are not referenced. Lundqvist claims a x4 over-estimate of dose at forward angles and a x 1/2 underestimate of dose at backward angles. Lundqvist neutron dose transmission results are presented here as figures 5-8. Note that the neutron sources are neutrons from the bombardment of copper. Lundqvist has also included in his notes similar curves for C and Pb targets. Lundqvist's

results at 200 MeV are within a factor of 2 from those of Alsmiller's et al.[7]

H.A.Smith[9] has reinterpreted Alsmiller's calculations[6] in a manner useful for angular interpolations. Also, he has some unpublished results from Alsmiller showing neutron energy spectra from 200 MeV protons on Al, Cu and C at 0-30° and 60°-90°.

Braid et al[10] have also used the Bertini-Alsmiller data to calculate shielding properties at the same polar angles as Alsmiller et al[6] and Lundqvist.[8] However, their calculations predict doses x1/6 that of Alsmiller at 200 MeV and x1/3 those of Lundqvist at 200 and 400 MeV respectively, at R=3m, thickness of 800 g/cm^2, and a polar angle between 0° and 30°. Braid and O'Brien were surprised about these discrepancies when contacted by phone around November 1986 but were not interested in reviewing their calculations.

Stevenson[11], in his review, discusses the problem of lateral neutron shielding. He has numerous references in it. While of no use when designing shielding for a medical facility, they may be very useful in other circumstances.

WALLS AND ROOF SHIELDING

The shielding calculations shown here are approximate. They are based on a very simple model to extend Alsmiller et al[6] work for shielding neutrons from stopping 200 MeV protons in aluminum, to 250 MeV protons stopping in aluminum and other materials.

To correct the curves given in figure 2 for 250 MeV protons stopping in aluminum to 250 MeV protons stopping in other materials, the following assumptions were made.

a. The neutron energy spectra produced by 200 MeV and 250 MeV protons stopping in different media are not significantly different from those of 200 MeV protons stopping in aluminum at corresponding polar angle intervals.

b. For thick walls, the evaporation neutrons do not contribute measurably to the dose equivalent on the outside of the shield.

Then,

c. The dose equivalent outside the shield depends on neutron production only.

d. The curves in figure 2 may be used for all target materials after suitable corrections for neutron production.

Furthermore, it is assumed that the curves in figure 2 may be scaled from one type of shielding material to another one scaling their thicknesses by their neutron mean free paths. The effect of placing steel in a hydrogeneous medium may be estimated from the work of Alsmiller and Barish[12], see figure 9.

Corrections for Target Material and Proton Energy

The correction factors for various target materials are calculated as follows,

$$R(m,\Delta\theta) = \frac{P(250,\ m)}{P(200,\ Al)} \times \frac{N(250,\ m,\Delta\theta)}{N(200,\ Al,\ \Delta\theta}$$

where,

$P(Ep, m)$ = probability of non-elastic scattering for a proton of incident energy Ep, stopping in medium "m", Ep = 250 or 200 MeV,[14]

$N(Ep, m, \Delta\theta)$ = average number of direct interaction (cascade) neutrons produced per ster-radian produced by protons of energy Ep, interacting with nuclei of medium "m" and scattered into the polar angular region $\Delta\theta = \theta_1 - \theta_2$,[4]

and

$R(m, \Delta\theta)$ = multiplicative factor for medium "m" and angular regions $\Delta\theta$, when using the curves in figure 2, drawn for 200 MeV protons stopping in Al.

The first ratio relates to the change in probability of making a non-elastic interaction before stopping and the second ratio refers to the neutron production multiplicities at 250 MeV in the material in question and at 200 MeV in aluminum.

The results of these calculations appear in Table I. Should a 250 MeV beam stop in muscle tissue (water), no corrections are necessary when using figure 2. On the other hand, without a body or a phantom, the proton beam in a treatment room would stop in the wall ($CaCO_3$) and neutron production would increase by 1.3.

TABLE I

250 MeV Protons. R(m,Δθ) for Various Elements and Compounds

Material	P(250)	N(250, m, Δθ)				R(m, Δθ)			
Notes	a	0-30° b	30-60° b	60-90° b	90-180° b	0-30°	30-60°	60-90°	90-180°
C	.400	.217	.344	.241	.089	1.2(4)	1.3(2)	1.3(2)	1.0(6)
O	.375	.254	.357	.232	.102	1.3(7)	1.2(9)	1.2(0)	1.1(4)
Al	.375	.247	.393	.273	.167	1.3(3)	1.4(2)	1.4(2)	1.8(7)
Cr	.351	.249	.432	.328	.155	1.2(5)	1.4(6)	1.5(9)	1.6(2)
Fe	.341	c	c	c	c	c	c	c	c
Cu	.341	.273	.434	.328	.189	1.3(3)	1.4(3)	1.5(5)	1.9(2)
W	.314	.269	.421	.320	.220	1.2(1)	1.2(8)	1.3(9)	2.0(6)
Pb	.307	.243	.430	.345	.223	1.0(7)	1.2(7)	1.4(6)	2.0(4)
Polyethylene	.308	d	d	d	d	0.9(6)	1.0(2)	1.0(3)	0.82
Polystyrene	.348	d	d	d	d	1.0(8)	1.1(6)	1.1(6)	0.92
Water	.302	e	e	e	e	1.1(0)	1.0(4)	0.97	0.92
$CaC0_3$	.367	.245	.369	.253	.110	1.2(9)	1.3(1)	1.2(8)	1.2(0)

	N(200, Al, Δθ)								
Material	P(200)	0°-30°	30°-60°	60°-90°	90°-180°				
Al	.287	.243	.361	.252	.117	-	-	-	-

Notes:
a from Ref. 14
b from Ref. 4
c use Cu data
d use C data.
e use O data.

Neutron Mean Free Paths for Some Shielding Materials

When space, money or both are at a premium, materials other than ordinary (light) concrete may be used. Table II gives neutron mean free paths as a function of polar angle for various types of shielding materials. To use this Table II, the abscissa in figures 2 and 5 through 8 must be first converted from g cm^{-2} units to λ mean free path units. Then, the curves become universal. The mean free paths are calculated using cross-sections from BNL-325,[13] the energy spectra shown in ref. 6, and shielding composition from Awschalom et al.[15] For the heavy concrete, the composition was reformulated for ρ = 3.4 g cm^{-3}. The cross-sections for the polar angles 0-30, 30-60, 60-90, and 90-180 degrees were calculated at E_n = 190, 110, 66, and 30 MeV respectively.

TABLE II
Neutron Mean Free Path for Different Materials and Polar Angular Region

Material	Ordinary Concrete	Compacted Soil	Ilmenite Concrete	Steel	Pb
Density g cm^{-3}	2.3	1.9-2.0	3.4	7.8	11.3
0°-30°	104(18)	106(21)	118(12)	139(7.0)	219(7.6)
30°-60°	93(16)	94(19)	107(11)	126(6.3)	204(7.1)
60°-90°	73(13)	74(15)	88(9.1)	112(5.6)	192.(6.7)
90°-180°	54(9)	54(11)	69(7.2)	94(4.8)	181(6.3)

The mean free paths are given in g cm^{-2} and in (inches).

Uncertainties in Shielding Design

Before using the curves in figure 2 one should ask the question: how accurately do they predict neutron doses?

One answer may be found in figure 1. In it, the greatest discrepancy between measurements and calculations is a very conservative factor of 3. This difference not only includes possible neutron spectra uncertainties but also the uncertainties in neutron activation cross-sections and experimental uncertainties. Hence, a dose safety factor of 4 has been used for these calculations at Fermilab in an attempt to also include a correction for the changes in energy spectra and thus mean free paths of the outgoing neutrons albeit what was said on pages 4 and 5. The additional factor of 4/3 comes from a rough interpolation using Lundqvist[8] calculations.

Dose equivalent at Zero Degrees

The neutron dose equivalent fluence is peaked at small forward angles and small depths into the shield. As the beam penetration continues, the forward peak looses its sharpness but the peak still remains well visible at all practical shielding thicknesses.[16]

Polar Angle Interpolations

Curves from Alsmiller[6] and Lundqvist[8] address the problem of average dose in four polar angle intervals (0°-30°, 30°-60°, 60°-90° and 90°-180°). But, in practical cases, it is very often necessary to be able to estimate shielding requirements at intermediate angles. It should be clear that the exercise that follows makes the best out of a very difficult situation. Recall that the parametrization

of neutron production by Alsmiller et al[4] is for the four polar angular regions listed above. Then, using the arguments of H.A.Smith[9], one will first define cos θ_{eff} as follows,

$$\cos\theta_{eff} = \int_{\theta_1}^{\theta 2} \cos\theta \, d\Omega \Big/ \int_{\theta_1}^{\theta_2} d\Omega = (\cos\theta_1 + \cos\theta_2)/2$$

Then, for a given shielding thickness, it is possible to plot R^2 Dose vs cos θ_{eff}. Interpolation between points is slightly questionable but the extrapolations to zero and to 180 degrees is left to the readers imagination.

Polar angle interval (degrees)	0/30	30/60	60/90	90/180
θ_{eff} (degrees)	21	47	75	120
cos θ_{eff}	.93	.68	.26	-.50

NEUTRON DOSE LEAKAGE THROUGH LABYRINTHS

Because of the importance to the reactor industry there are many modern computer codes available to calculate neutron dose leakage through ducts and larger penetration[17-19]. There are also a number of measurements around high energy accelerators that attest the accuracy with which these codes predict the high energy interaction experimental results[20-23]. Some comparisons of the most popular method of neutron dose leakage calculations, using the dose albedo concept, can also be found for the reactor energy region[22,24,25]. There are calculations comparing the MORSE code with measurements and the results of the albedo model[26], and the AMC code and measurements[22].

Actually, it is interesting that the monoenergetic dose albedo model should give results as good as they are in view of the changes in neutron energy spectra as the neutrons flow from leg to leg of the labyrinth[27,28].

Calculating Neutron Dose Equivalent Leaks

The agreement between measurements and calculations deteriorate slowly, leg by leg. By the third leg the albedo model may be underestimating the leak dose by a factor of 2-3. Furthermore, the guidelines given below assume that the dose attenuation in the third and farther legs should be the same as in the second, this should not be quite the case from figure 9, ref. 28.

Labyrinth calculations have two parts: the dose equivalent fluence (H) incident on the axis of the first leg at the entrance, and the dose equivalent transmission (attenuation) by the labyrinth itself.

The guidelines offered for labyrinth dose leakage attenuation are based on the published work of Gollon and Awschalom[29] and a recent survey made by Stevenson[30].

Calculation of Dose Equivalent Fluences About a Point Source

For a labyrinth, cascade and evaporation neutrons might be significant. Therefore, dose equivalent/(incident proton sr) was calculated for cascade neutrons for seven different target materials and four polar angular regions as well as for the same materials but for evaporation neutrons. Both calculations were done for incident protons of 250 MeV.

The neutron fluence to dose equivalent conversion factors were taken from NCRP #39.[31] The neutron energy spectra (neutrons MeV^{-1} sr^{-1}) were calculated using the algorithm and constants given in ref. 4. The results are given in Table III.

To use these numbers multiply them by the solid angle corresponding to 1 cm^2 at the distance of interest and by the number of incident protons.

TABLE III
Dose Equivalent Fluence(H)
250 MeV Incident Protons, Cascade and Evaporation Neutrons

Units: rem x $(inc\ prot)^{-1}$ x $(sr)^{-1}$

Material	Polar Angular Interval 0-30	30-60	60-0	90-180	Evaporation
C	.53(-8)	.28(-8)	.14(-8)	.24(-9)	.43(-9)
O	.62(-8)	.27(-8)	.12(-8)	.26(-9)	.42(-9)
Al	.58(-8)	.30(-8)	.14(-8)	.38(-9)	.58(-9)
Cr	.52(-8)	.31(-8)	.16(-8)	.40(-9)	.16(-8)
Cu	.58(-8)	.30(-8)	.16(-8)	.46(-9)	.24(-8)
W	.51(-8)	.28(-8)	.15(-8)	.53(-9)	.61(-8)
Pb	.46(-8)	.27(-8)	.16(-8)	.54(-9)	.67(-8)
Average	.54±.05 (-8)	.29±.02 (-8)	.15±.02 (-8)	.40±.12 (-9)	———

The number in parenthesis is the power of ten multiplying the number on the left.

Dose Transmission Along Labyrinths

Using the concept of labyrinth unit length introduced by Gollon and Awschalom[29], the x-axis of the dose attenuation curves is marked in units of $\sqrt{A}$ where A is the cross-sectional area of the labyrinth. This concept was tested over a 1:1 to 4:1 ratio of labyrinth cross-sections[29].

Figures 10 and 11 are taken from ref. 30. In figure 10, the curve labelled "point" refers to a point source on the axis of first leg of the labyrinth. For a point not on this axis the attenuation is a function of the location of the point. In figure 12, a much larger attenuation for a source point at 45 degrees from the leg axis is shown. There is no good experimental data to solve this discrepancy.

Figure 11, is given as a typical neutron dose attenuation curve for legs 2 and following ones. In figure 11, two dashed curves are shown, the lower ones represents the albedo dose model and the upper one some results using the SAM-CE code.

Figure 12, from reference 29, gives some variants of the typical cul-de-sac. Figure 13, ref. 29, shows the effects of using conventional cul-de-sacs (figure 13a), giving the results of placing the cul-de-sac in various locations and being made of various depths.

The exit dose equivalent, then, is given by

H(exib) = H(input from table III) x labyrinth attenuation.

Some Comments

1. The labyrinth calculations assume that the walls are thick.
2. Many short legs are more effective than fewer longer ones.
3. Cul-de-sacs should be deep, ~$\sqrt{A}$ or they are not very useful.

Acknowledgement

To Dr. Lundqvist for allowing me to use illustrations from his unpublished report, ref. 8, and to Dr. R.G. Alsmiller for some very useful conversations. Ms. Marion Richardson and Ms.Claudia Foster typed and corrected this manuscript many a time. Last but not least are my thanks to Michael Allen who, playing the role of Socrate's horsefly, got me to finish this TM.

REFERENCES

1. C.H.Distenfeld, Shielding Measurements-200 MeV Linac, BNL-18025, BNL(1973).

2. J.W.Wachter, M.R.Burrus, W.A.Gibson, Neutron and Proton Spectra from Targets Bombarded by 160 MeV Protons, Phys.Rev.161, 971(1967).

3. H.W.Bertini, Phys.Rev. 131, 1801(1963), erratum Phys.Rev.138, AB2(1965), ORNL-TM-1225(1965), ORNL-3844(1966), Trans.Am.Nucl.Soc., Wash., D.C., Nov.15-18, 1965, p.634.

4. R.G.Alsmiller, M.Leimdorfer, J.Barish; Analytical Representation of Non-elastic Cross Sections and Particle-Emission Spectra from Nucleon-Nucleus Collisions in the Energy Range 25 to 400 MeV, ORNL-4046 (April 1967).

5. S.Ban, H.Hirayama, K.Katoh, Measurement of Secondary Neutron Fluxes Around Beam Stop for 500 MeV Protons, Nucl.Instr.Meth. 184, 409 (1982).

6. R.G.Alsmiller, R.T.Santoro, J.Barish; Shielding Calculation for a 200 MeV Proton Accelerator and Comparisons with Experimental Data, Particle Accelerators 7, 1 (1975), also available as ORNL-TM-4754 (2/1975).

7. R.G.Alsmiller, J.Barish, R.T.Boughner, and W.W.Engle; Shielding Calculations for a 200 MeV Proton Accelerator, ORNL-4336, Dec.1968.

8. H.Lundqvist, Radiation Protection Calcullations for a Proton Cyclotron in the Energy Range 100-400 MeV, Dept. of Radiobiology, the Gustaf Werner Institute, University of Uppsala, Uppsala, Sweden, report GWI-R 18/72.

9. H.A.Smith, Shielding Calculations and Beam Dump Shielding Design Considerations for the Indiana University Cyclotron Facility, Indiana University Cyclotron Facility Internal Report No.74-6, May, 1974.

10. T.H.Braid, R.F.Rapids, R.H.Siemssen, J.W.Tippie and K.O'Brien, Calculations of Shielding for Large Cyclotrons, IEEE Trans.Nucl.Science NS-18, 824(1971).

11. G.R.Stevenson, Shielding at Proton Energies of less than 3 GeV, CERN-TIS-RD/IR/86-08.

12. R.G.Alsmiller and J.Barish, Shielding Against the Neutrons Produced When 400 MeV Electrons are Incident on a Thick Copper Target, ORNL-TM-4060.

13. D.J.Hughes and R.B.Schwartz, Neutron Cross-Sections, 2nd Ed. BNL-325 (7-1-85).

14. J.F.Janni; Proton Range-Energy Tables, 1 keV - 10 GeV, Part I, compounds, Atomic Data and Nuclear Data Tables 23, 150-339 (1982), Part II, elements, ibid, pp 341-529.

15. M.Awschalom, T.Borak, and P.G.Gollon, Chemical Composition of Some Common Shielding Materials, Fermilab TM-168 (5-2-69).

16. R.G.Alsmiller, The Lateral Spread of High Energy (≤400 MeV) Neutron Beams and Earth Shine, Nucl. Instr. Meth. 89, 53 (1970).

17. F.Gervaise and M.M. d'Hombres, Variante du Programme ZEUS Applique a des Problemes des Tunnels, CEA-Report-N-933 (1968).

18. R.E.Marker and V.R.Chain, AMC A Monte Carlo Coole Utilizing the Albedo Approach for Calculating Neutron and Capture Gamma Ray Distributions in Rectangular Concrete Ducts, ORNL-3964 (1967).

19. E.A.Straker, P.N.Stevens, D.C.Irving and J.R.Cain. A Multigroup Neutron and Gamma-Ray Monte Carlo Transport Code, ORNL-4585 (1970).

20. G.R.Stevenson and D.M.Squier, An Experimental Study of Attenuation of Radiation in Tunnels Penetrating the Shield of an Extracted Beam of the 7 GeV Proton Synchrotron Nimrod, Health Physics 24, 87 (1973).

21. W.Schimmerling and M.Awschalom Neutron Flux in a Labyrinth Due to 3 GeV Proton Beam Incident on Lead, Proc. 1969 Particle Accel.Conf., Wash. 1969, Vol.I, p.604.

22. R.G.Alsmiller and E.Solomito, The Transport of Neutrons Produced by 3 GeV Proton-Lead Nucleus Collisions Through a Labyrinth and Comparison with Experiment, ORNL-TM-2560.

23. J.D.Cossairt, J.G.Couch, A.J.Elwyn, W.S.Freeman; Radiation Measurements in a Labyrinth Penetration at a High Energy Proton Accelerator, Health Physics 49, 907 (1985).

24. R.E.Maerker and F.J.Muckenthaler, Calculation and Measurement of the Fast Neutron Differential Dose Albedo for Concrete, Nucl. Sci. Eng. 22, 455 (1965).

25. R.E.Maerker and F.J.Muckenthaler, Monte Carlo Calculations, Using the Albedo Concept, of the Fast-Neutron Dose Rates along the Center Lines of One-and Two-Legged Square Concrete Open Ducts and Comparison with Experiment, Nucl.Sci.Eng.27, 423 (1967).

26. Ye Sizong, The Calculation of the Neutron Transmission Through the Access Way of A High-Energy Accelerator Installation (using the MORSE code) CERN Report HS-RP/066/PP (Feb. 8, 1982).

27 H.G.Vogt, Monte Carlo Calculations of the Neutron Transmission through the Access Ways of the CERN Super Proton Synchrotron, CERN 75-14, Nov. 6, 1975

28. R.E.Maerker and F.J.Muckenthaler, Neutron Fluxes in Concrete Ducts Arising from Incident Epicadmium Neutrons: Calculations and Experiments, Nucl.Sci.Eng.30, 340 (1967)

29. P.J.Gollon and M.Awschalom, Design of Penetrations in Hadron Shields, IEEE Trans.Nucl.Sci. NS-18, 741 (1971).

30. G.R.Stevenson, Neutron Attenuation in Labyrinths, Ducts and Penetrations, CERN-TIS-RP/IR/86-07, February 10, 1986.

31. Basic Radiation Protection Criteria, NCRP Report No. 39, National Council on Radiation Protection and Measurements, Washington, DC, January 15, 1971.

General Reference

H.Wade Patterson and Ralph H. Thomas, Accelerator Health Physics, N.Y.: Academic Press, 1973.

FIGURE CAPTIONS

1. Reference 6, figure 3 (Alsmiller, Santoro, Barish) Activation per incident proton as a function of radius in water.
2. Same as figure 1, but figure 6 and R^2 Dose Equivalent[(cm^2 rem) per (incident proton)] as a function of radius in ordinary coverete (density = 2.3 g/cm^3) for various polar angles.
3. Reference 8, figure 1 (Lundqvist) yield [(neutrons/MeV/sr)per(incident proton)] for 160 MeV protons incident on a thick carbon target.
4. Reference 8, figure 2, same, but for a thick copper target.
5. Reference 8, figure 4a. 100 MeV protons stopping in a thick copper target. Neutron dose equivalent [(rem/h)per(incident proton/sec)] at 1 mm from target, as a function of thickness of ordinary concrete(density=2.3 g/cm^3) for a various polar angles.
6. Same as figure 3, but figure 4b for 200 MeV protons.
7. Same as figure 4, but figure 4c for 300 Mev protons.
8. Same as figure 4, but figure 4d for 400 MeV protons.
9. Reference 12, figure 4 (Alsmiller and Barish)R^2 Dose Equivalent versus radius in units of mean free path.
10. Reference 30, figure 8, (Stevenson) neutron dose equivalent attenuation in the first leg of a labyrinth.
11. Reference 30, figure 10, neutron dose equivalent attenuation in legs 2 and subsequent ones.

12. Reference 29, figure 9 (Gollon and Awschalom) variants of conventional cul-de-sac.
13. Same as 12, but showing effect of placing conventional cul-de-sac in various locations and changing its length.

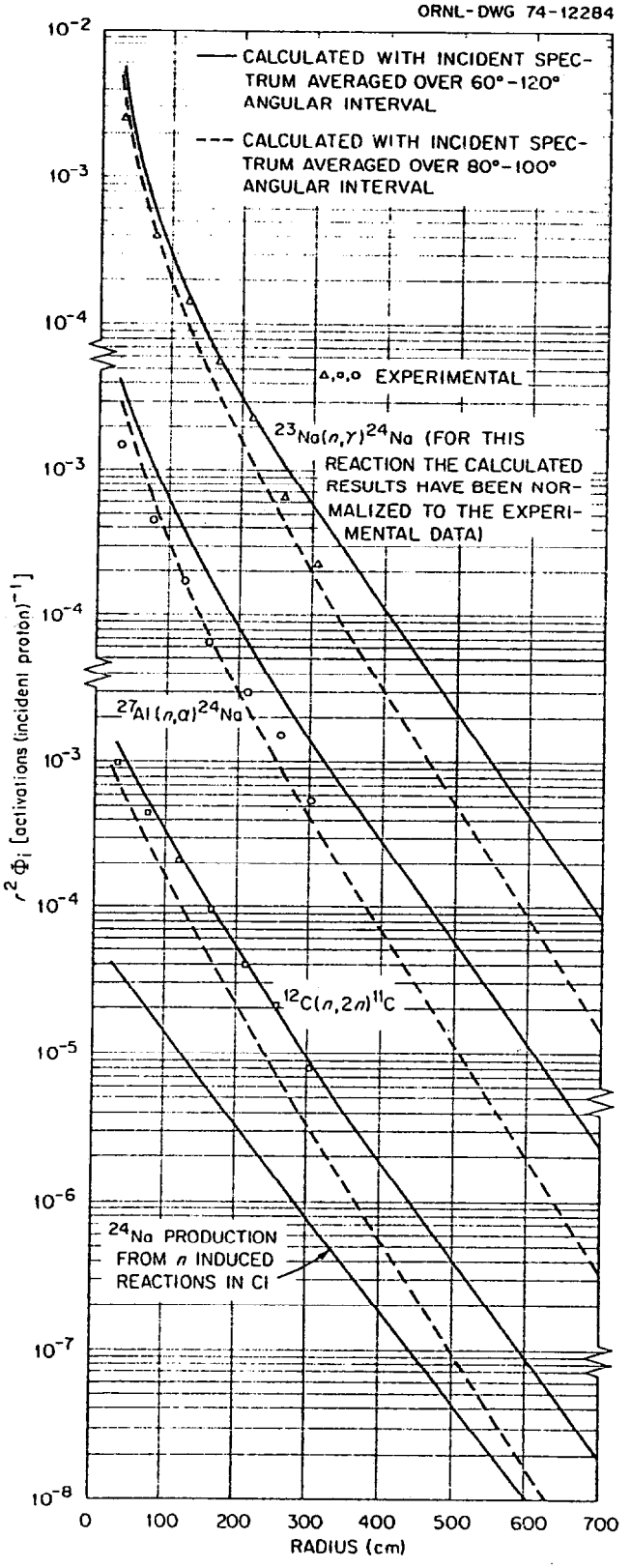

Fig. 1

Experimental and calculated activation data multiplied by r^2 vs radius in the water shield.

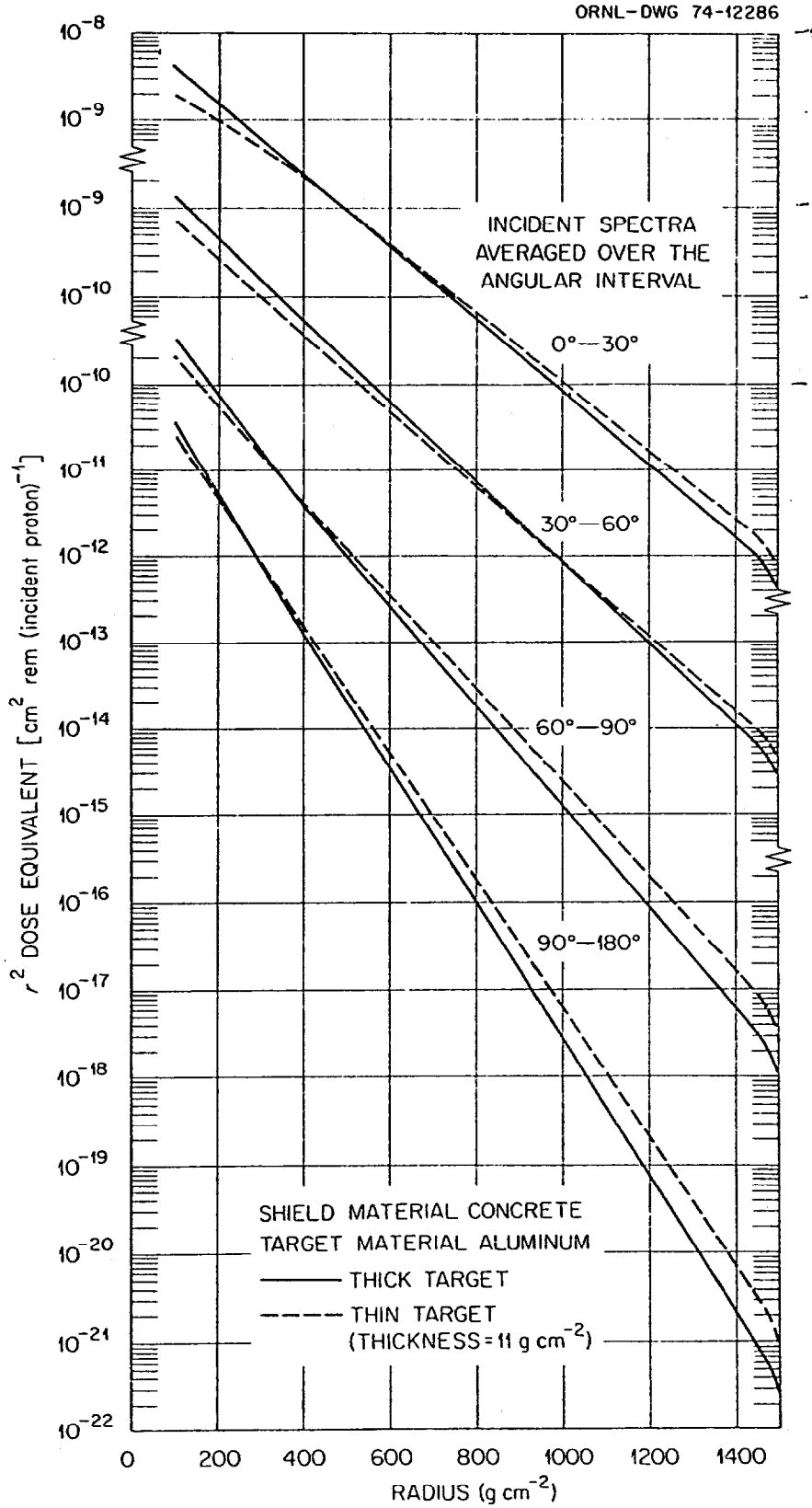

Fig. 2

Dose equivalent multiplied by r^2 vs radius in the concrete shield.

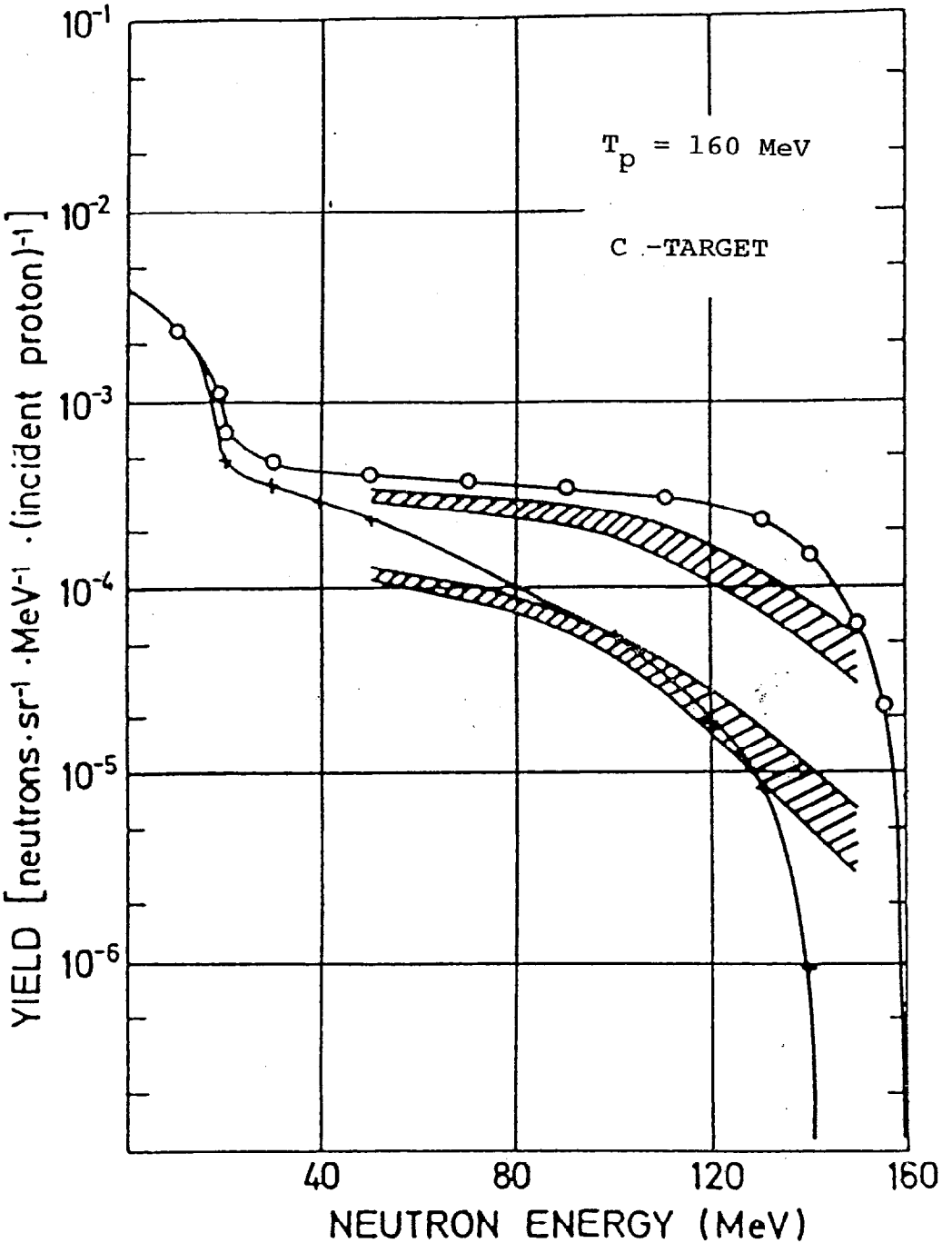

o calculated neutron spectrum in 0-30 degrees

\+ " " " " 30-60 "

▨ experimental " " from ORNL-TM-1781

Fig. 3

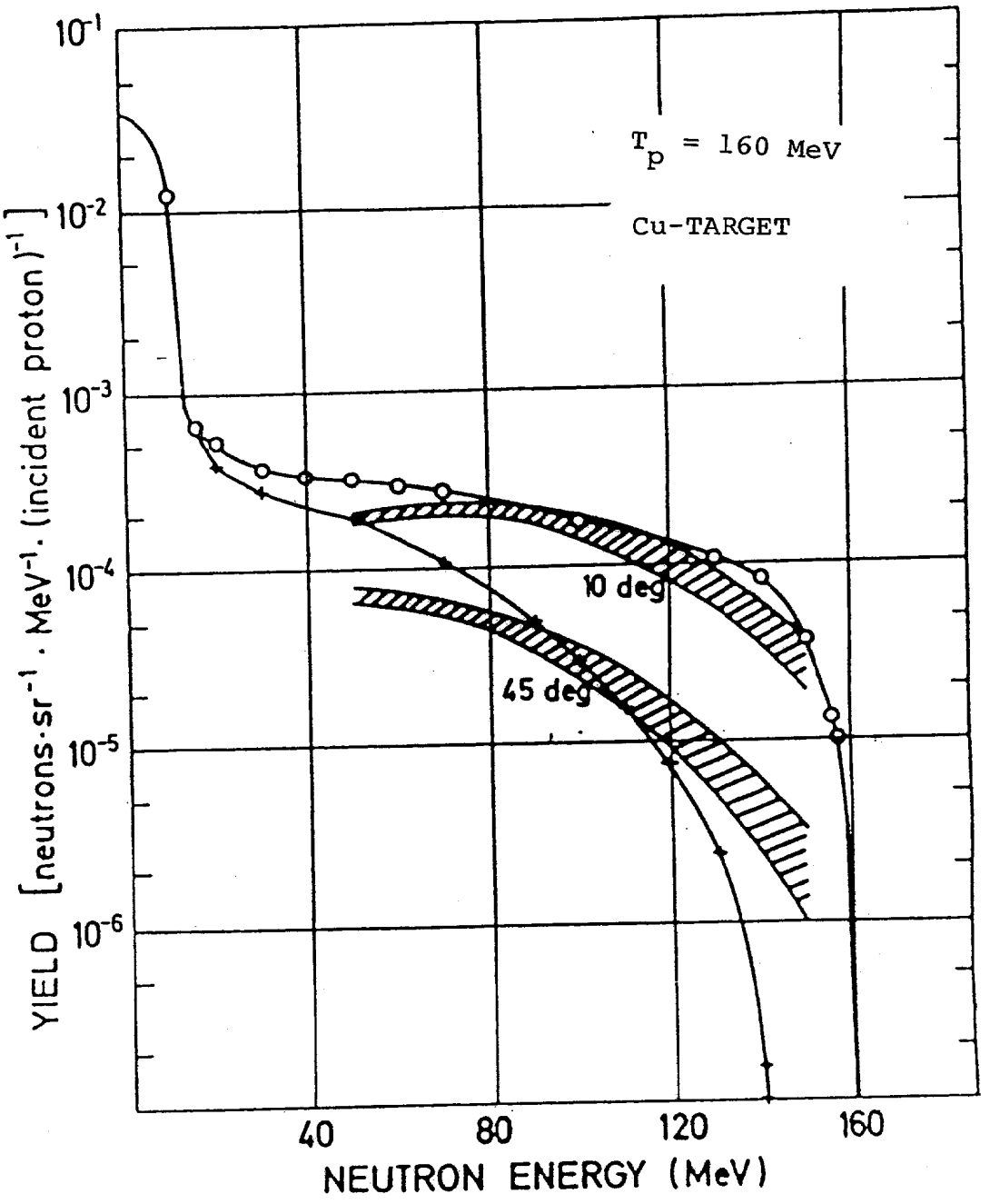

o calculated neutron spectrum in 0-30 degrees
+ " " " " 30-60 "
▨ experimental " " from ORNL-TM-1781

Fig. 4

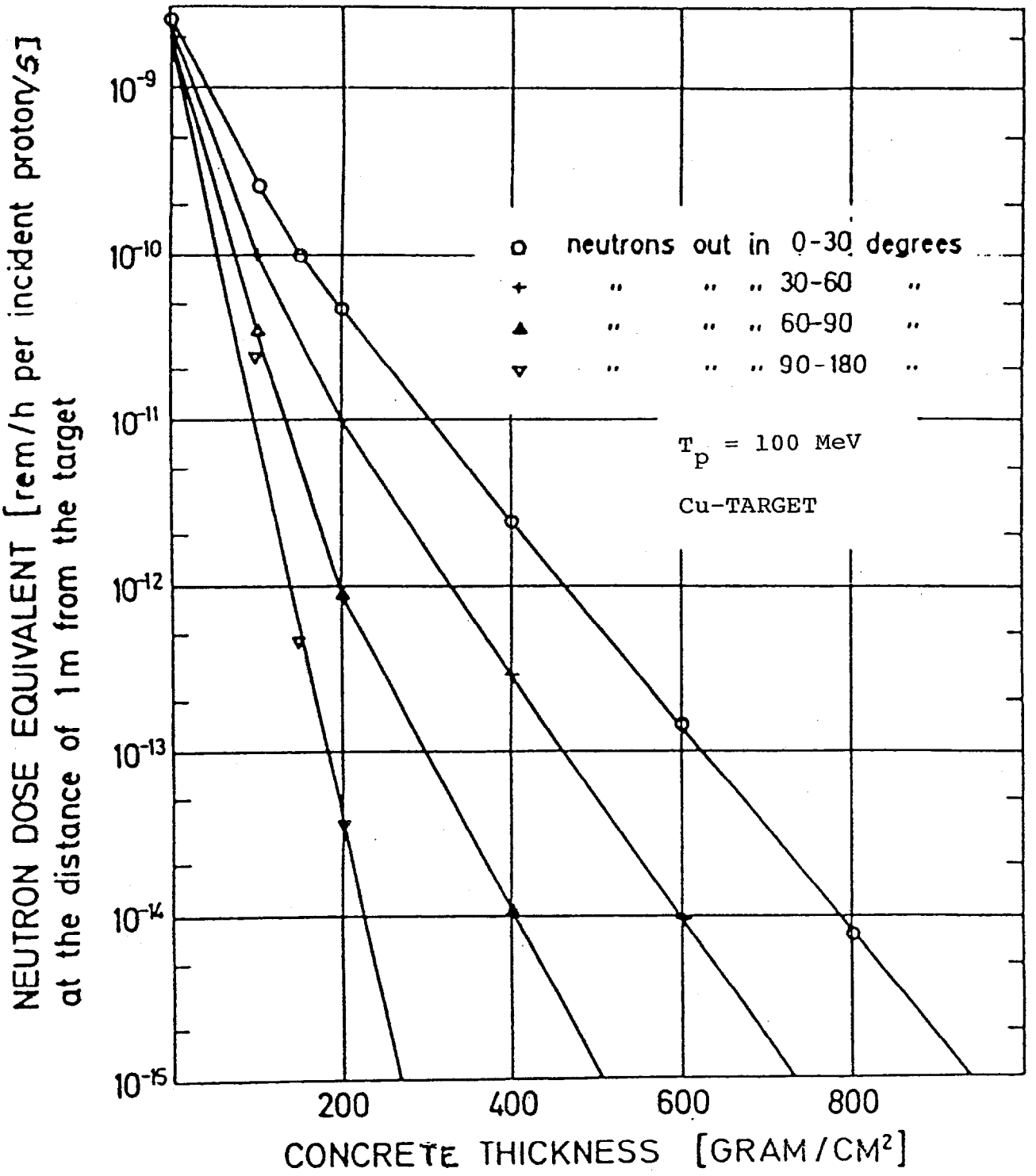
NEUTRON DOSE EQUIVALENT [rem/h per incident proton/s] at the distance of 1 m from the target
10⁻⁹
10⁻¹⁰
10⁻¹¹
10⁻¹²
10⁻¹³
10⁻¹⁴
10⁻¹⁵
200
400
600
800
CONCRETE THICKNESS [GRAM/CM²]
o neutrons out in 0-30 degrees
+ " " " 30-60 "
▲ " " " 60-90 "
▽ " " " 90-180 "
T_p = 100 MeV
Cu-TARGET

Fig. 5

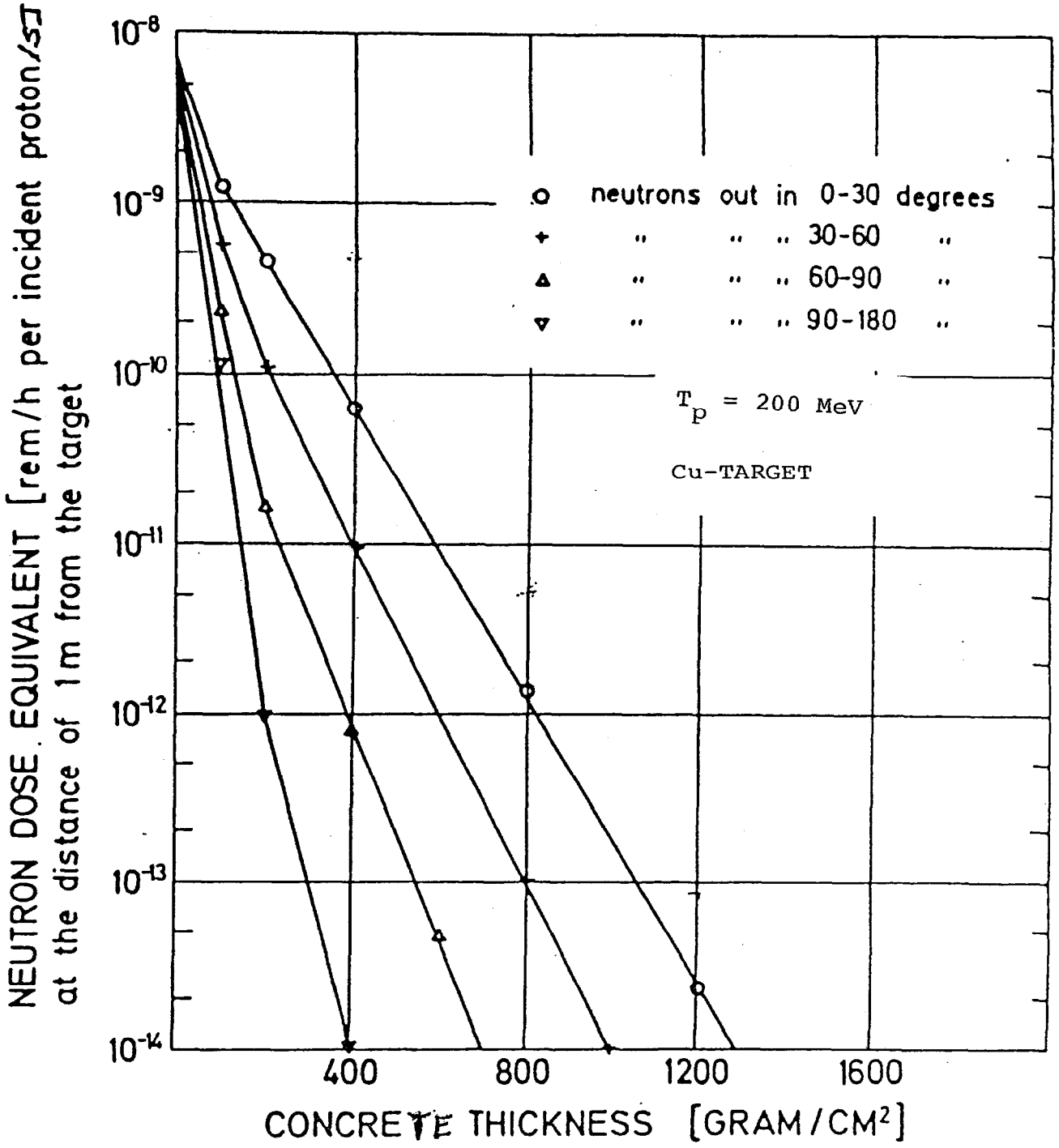
NEUTRON DOSE EQUIVALENT [rem/h per incident proton/sr] at the distance of 1m from the target
10-8
10-9
10-10
10-11
10-12
10-13
10-14
400
800
1200
1600
CONCRETE THICKNESS [GRAM/CM2]
neutrons out in 0-30 degrees
" " " 30-60 "
" " " 60-90 "
" " " 90-180 "
Tp = 200 MeV
Cu-TARGET

Fig. 6

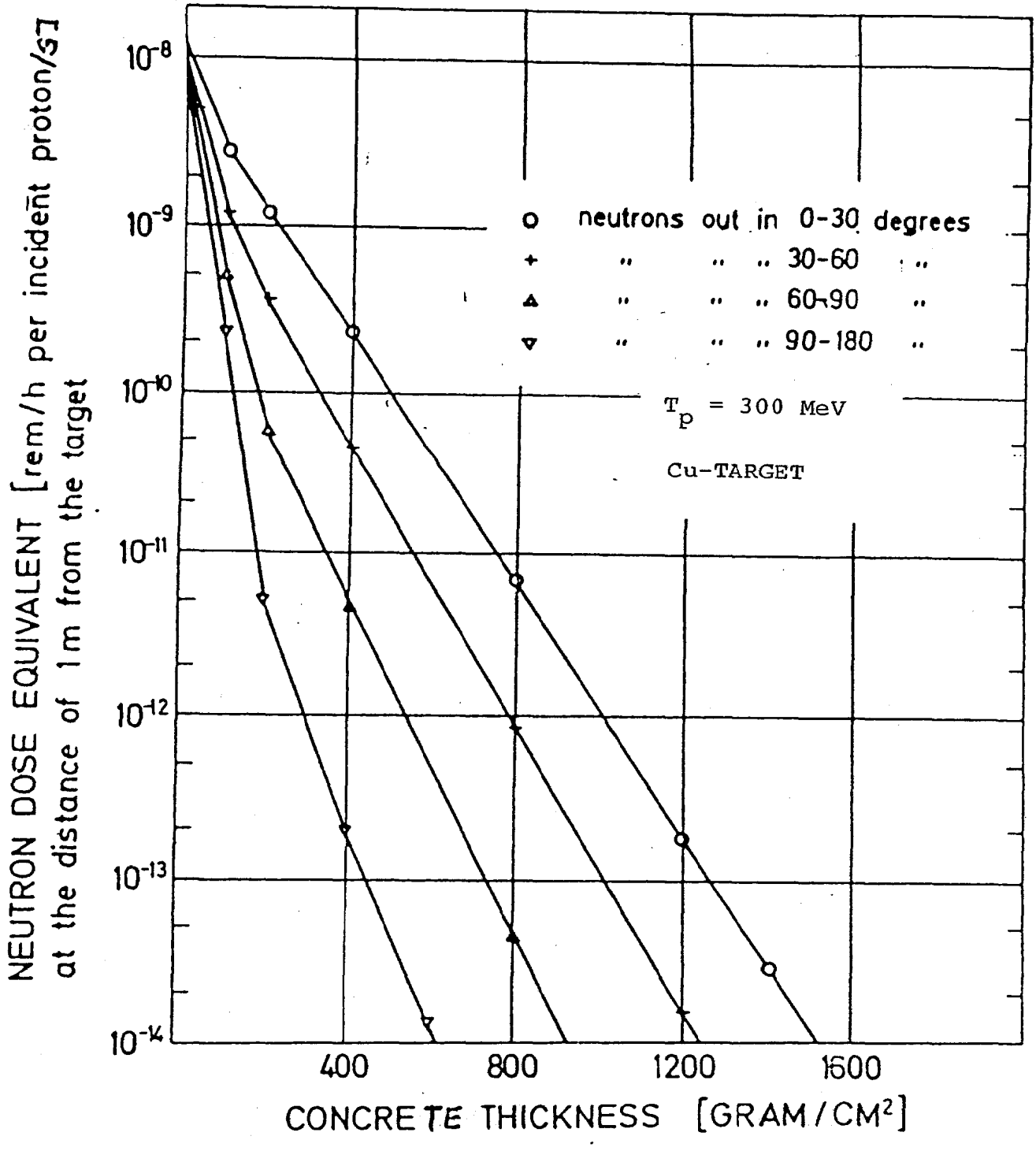
NEUTRON DOSE EQUIVALENT [rem/h per incident proton/sr]
at the distance of 1m from the target
10-8
10-9
10-10
10-11
10-12
10-13
10-14
400
800
1200
1600
CONCRETE THICKNESS [GRAM/CM2]
neutrons out in 0-30 degrees
" " " 30-60 "
" " " 60-90 "
" " " 90-180 "
Tp = 300 MeV
Cu-TARGET

Fig. 7

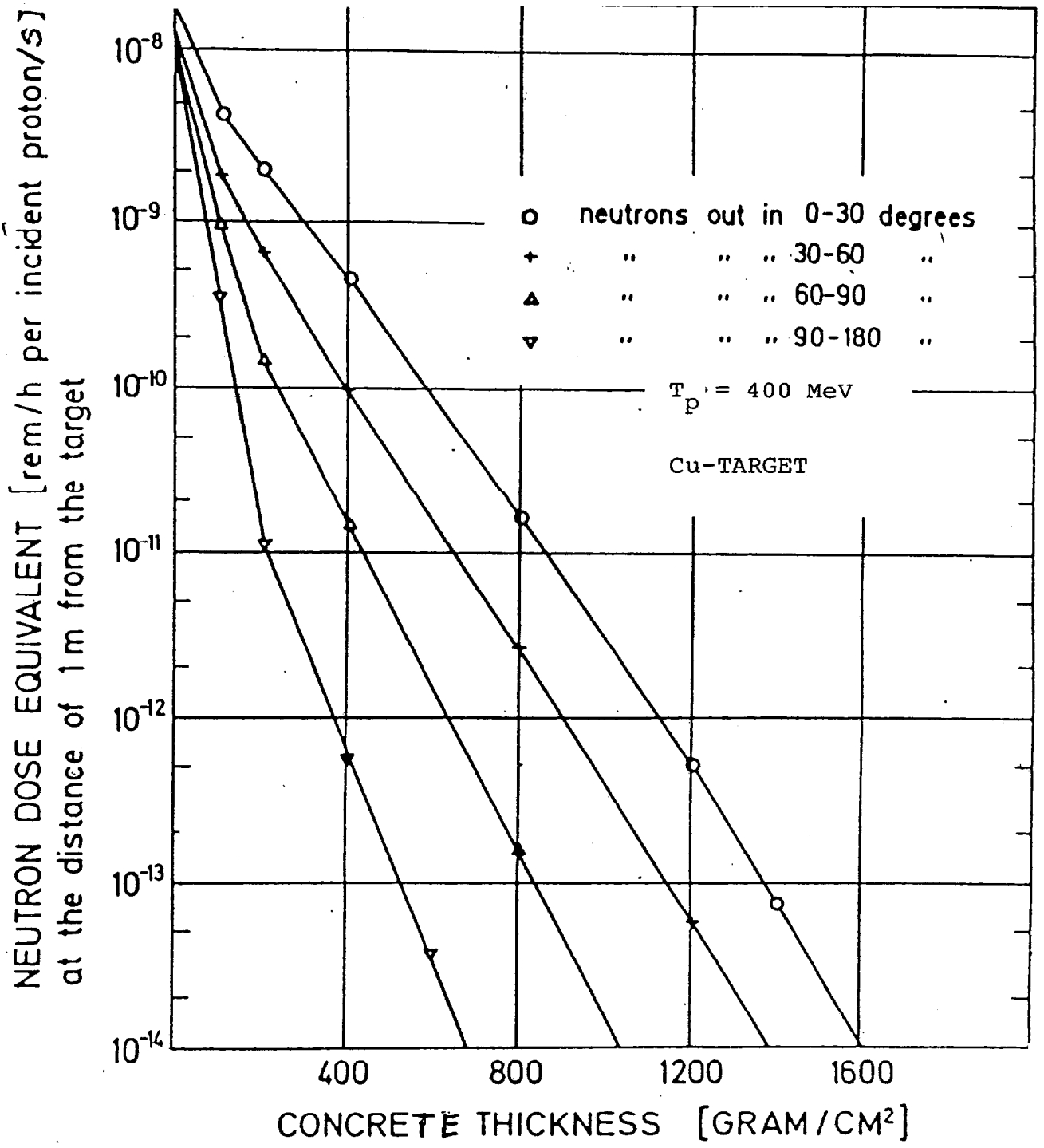
NEUTRON DOSE EQUIVALENT [rem/h per incident proton/s] at the distance of 1 m from the target
10-8
10-9
10-10
10-11
10-12
10-13
10-14
400
800
1200
1600
CONCRETE THICKNESS [GRAM/CM2]
neutrons out in 0-30 degrees
" " " 30-60 "
" " " 60-90 "
" " " 90-180 "
Tp = 400 MeV
Cu-TARGET

Fig. 8

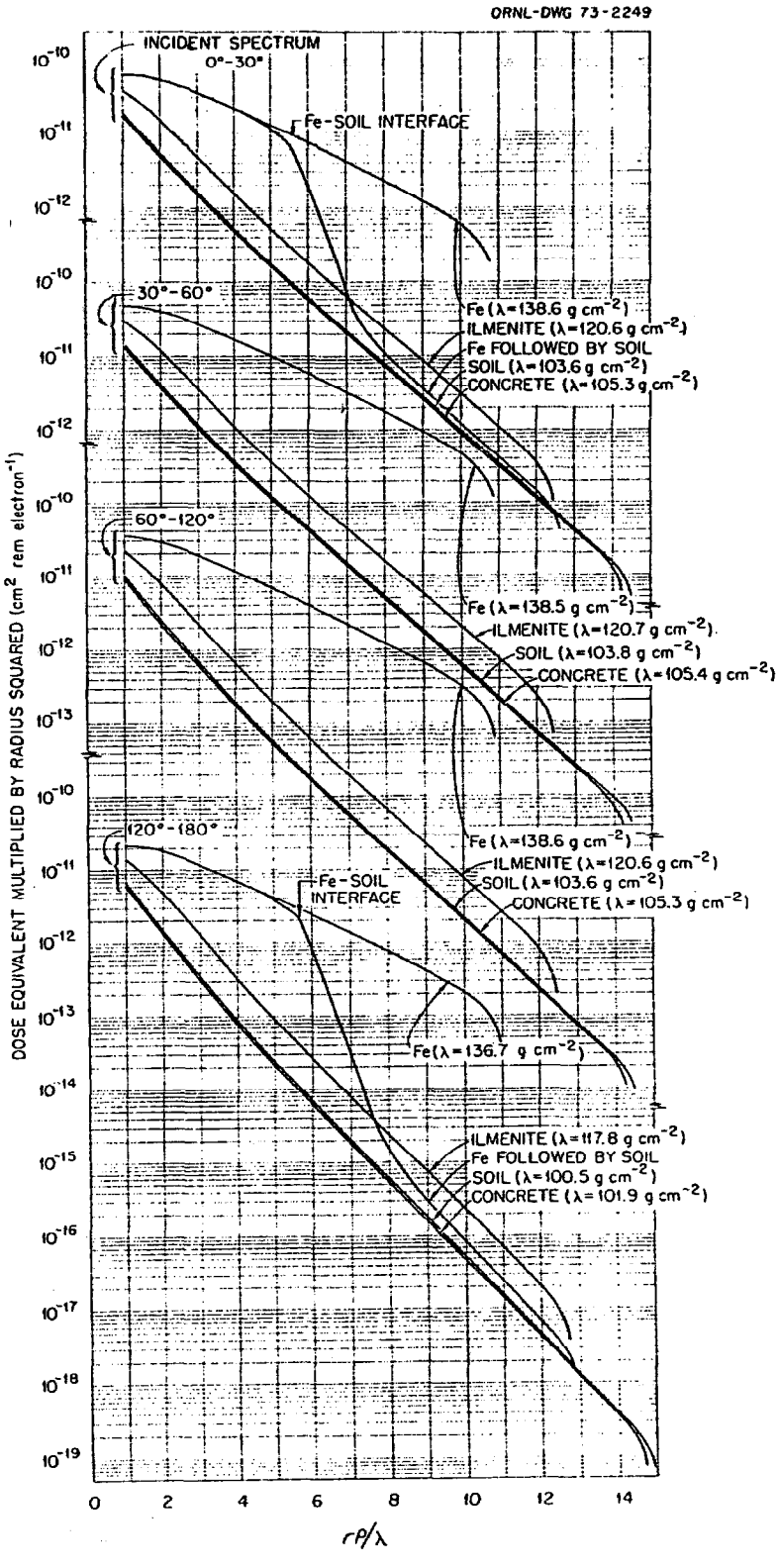

Fig. 9

Dose equivalent multiplied by the radius squared vs radius for a variety of incident spectra and shield materials. Note that the dose equivalent has been multiplied by the radius squared in cm^2, but the results are plotted against the radius measured in mean free paths.

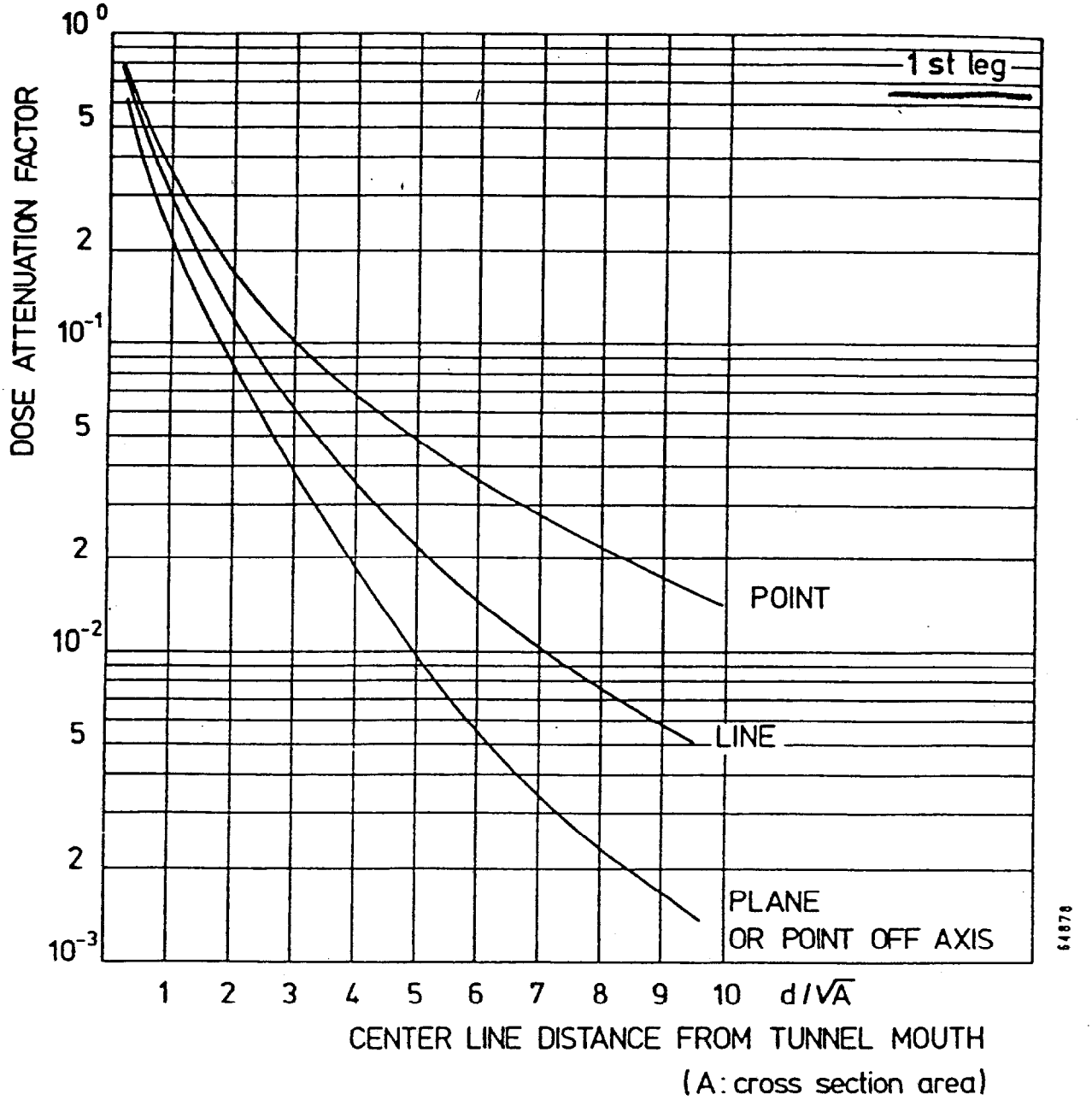
DOSE ATTENUATION FACTOR
10 0
5
2
10-1
5
2
10-2
5
2
10-3
1st leg
POINT
LINE
PLANE
OR POINT OFF AXIS
64878
1 2 3 4 5 6 7 8 9 10 d/√A
CENTER LINE DISTANCE FROM TUNNEL MOUTH
(A: cross section area)

FIG. 8

Fig. 10

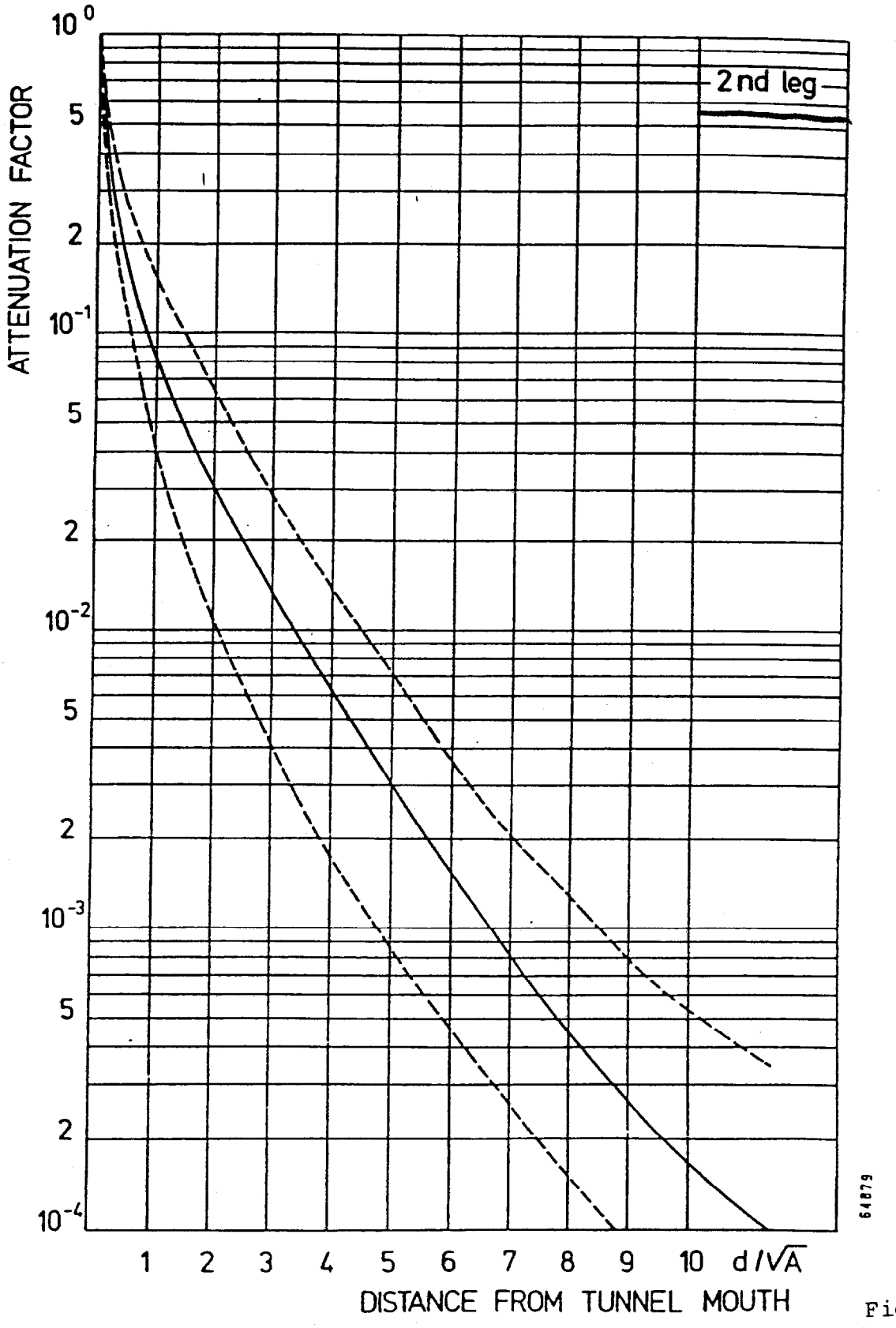
ATTENUATION FACTOR
10 0
5
2
10-1
5
2
10-2
5
2
10-3
5
2
10-4
2nd leg
1 2 3 4 5 6 7 8 9 10 d/√A
DISTANCE FROM TUNNEL MOUTH
64879

Fig. 11

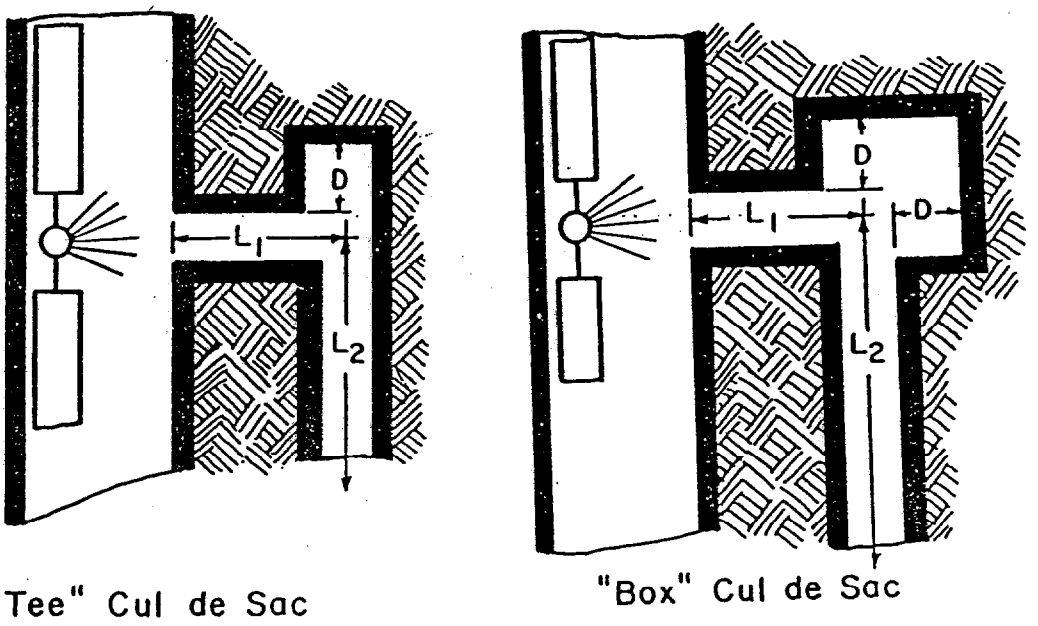

Novel cul-de-sac geometries.

Fig. 12

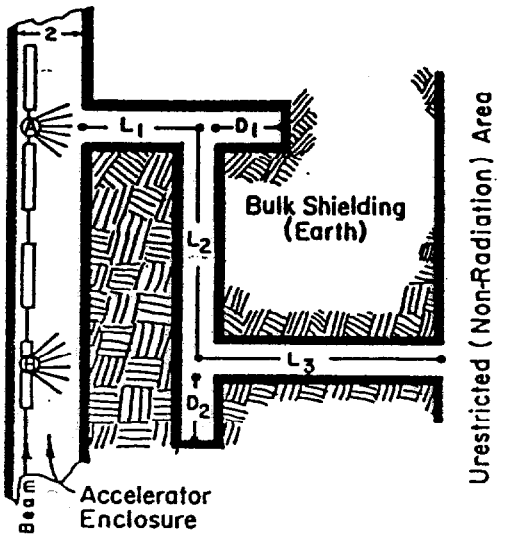
2
L1
D1
Bulk Shielding
(Earth)
L2
L3
D2
Beam
Accelerator
Enclosure
Unrestricted (Non-Radiation) Area

-a-

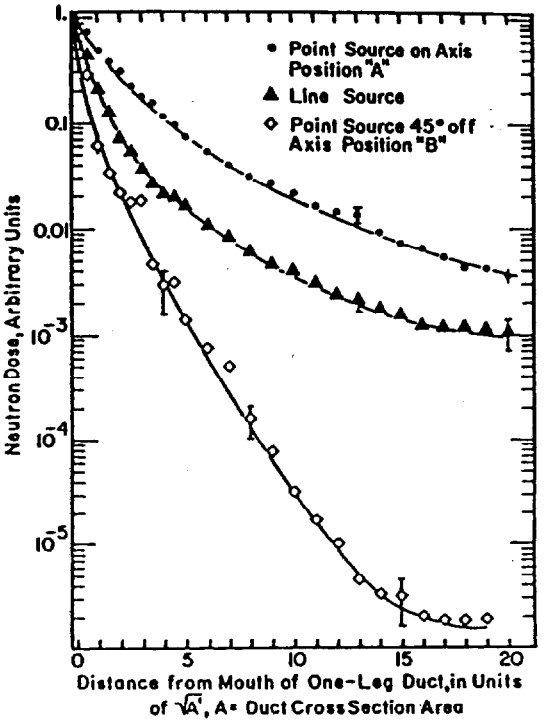
Point Source on Axis Position "A"
Line Source
Point Source 45° off Axis Position "B"
Neutron Dose, Arbitrary Units
Distance from Mouth of One-Leg Duct, in Units of √A, A = Duct Cross Section Area

-b-

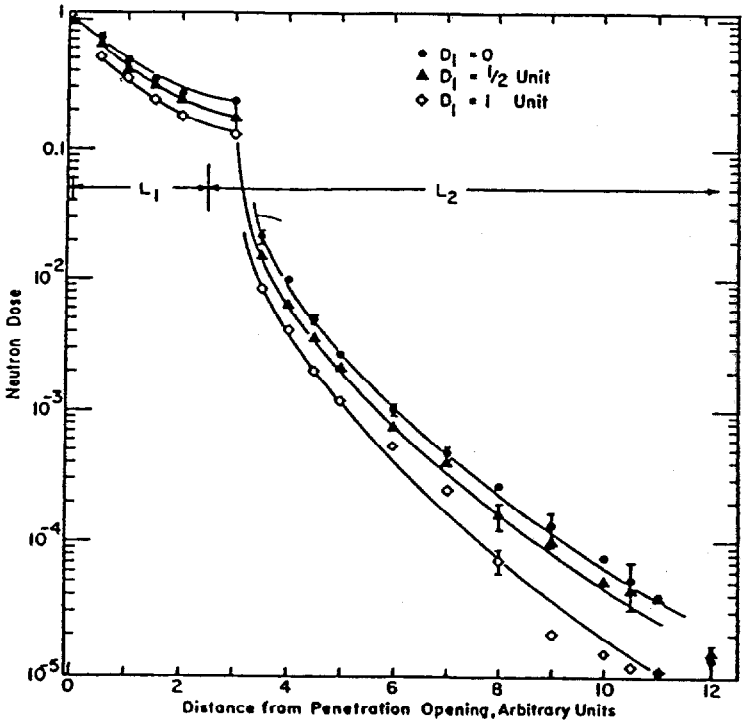
D1 = 0
D1 = 1/2 Unit
D1 = 1 Unit
L1
L2
Neutron Dose
Distance from Penetration Opening, Arbitrary Units

-c-

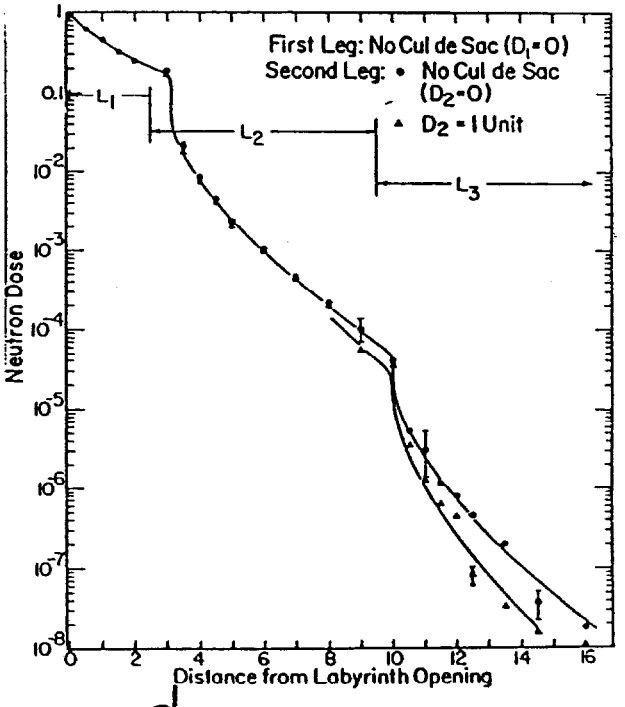
First Leg: No Cul de Sac (D1 = 0)
Second Leg: No Cul de Sac (D2 = 0)
D2 = 1 Unit
L1
L2
L3
Neutron Dose
Distance from Labyrinth Opening

-d-

Fig. 13